Solar Energy Materials & Solar Cells 133 (2015) 8–14

Contents lists available at ScienceDirect

Solar Energy Materials & Solar Cells

journal homepage: www.elsevier.com/locate/solmat

Theoretical analysis on effect of band offsets in perovskite solar cells

Takashi Minemoto*, Masashi Murata

Department of Electrical and Electronic Engineering, Ritsumeikan University, 1-1-1 Nojihigashi, Kusatsu, Shiga 525-8577, Japan

ARTICLE INFO

Article history:
Received 18 June 2014
Received in revised form
30 September 2014
Accepted 25 October 2014

Keywords:
Solar cells
Perovskite
Device simulation
Band offset
Buffer layer
Hole transport material

ABSTRACT

The effect of band offsets in $CH_3NH_3PbI_{3-x}Cl_x$ perovskite-based solar cells with planar junction configuration was analyzed using one-dimensional device simulator. As widely known in thin-film compound solar cells, the band offset between buffer/absorber layers is a decisive factor for carrier recombination at the interface, determining open-circuit voltage (V_{oc}). In this study, the impact of two kinds of band offsets, i.e., the conduction band offset of buffer (or blocking layer)/absorber layers and the valence band offset of absorber/hole transport material (HTM) were examined. When the conduction band of the buffer was lower than that of the absorber, the interface recombination became prominent and V_{oc} decreased. In contrast, when the conduction band of the buffer was higher than that of the absorber by more than 0.3 eV, the collection of photo-generated carriers, i.e. electron in this case, was impeded by the spike formed by the conduction band offset. Thus, the optimum position of the conduction band of the buffer was 0.0∼0.3 eV higher than that of the absorber. Also, the optimum position of the valence band of the HTM was derived to be 0.0∼0.2 eV lower than that of the absorber. These findings will be useful for new material choice and optimization of buffers and HTMs.

1. Introduction

Thin film solar cells based on lead methylammonium tri-iodide perovskite as an absorber have attracted considerable attention as low-cost and high efficiency organic-inorganic hybrid solar cells [1–9]. Initially, high efficiencies of over 10% were reported using perovskite absorbers with mesoporous scaffold layers [1–5]. After the promising results, a similar range of high efficiencies were reported by planar junction configuration, i.e., without the mesoporous structure [6–9]. Especially, high efficiencies of over 15% were reported using $CH_3NH_3PbI_{3-x}Cl_x$ and $CH_3NH_3PbI_3$ perovskite absorbers [7,8]. High light absorption coefficient [10] and long carrier diffusion length [2] should be the origin of the flexibility of the device architecture; namely, the mesoporous structure is not a requirement to achieve this level of high efficiency.

To achieve higher efficiency, the understanding of device operation mechanism is important. To this end, device simulation is useful, and conventional solar cells based on inorganic semiconductors such as silicon, CdTe, $Cu(In,Ga)Se_2$ (CIGS), and $Cu_2SnZn(S,Se)_4$ were widely analyzed by device simulators [11–21]. However, the detailed theoretical analysis of the perovskite solar cells using device simulation is few. The perovskite materials are organic-inorganic hybrid materials and have similar material properties with inorganic materials; especially low binding energy of exciton, and thus the exciton is Wannier-type [22]. Also, the device structures of the perovskite solar cells with planar junction and inorganic thin film solar cells, such as CIGS, are similar. The typical structure for the perovskite solar cells is transparent conductive oxide (TCO)/blocking layer (or buffer)/absorber/hole transport material (HTM)/metal back contact [7,8], and that of CIGS solar cells is TCO/buffer/absorber/metal back contact [23–25]. From the two facts, solar cell device simulator widely used in CIGS solar cells can be applied to the perovskite solar cells. In our previous study [26], we analyzed the effect of absorber and interface qualities and the optimum thickness of the absorber of the perovskite solar cells using the Solar Cell Capacitance Simulator (SCAPS) developed by University of Gent [27].

The CIGS solar cells are heterojunction solar cells, similar to the perovskite solar cells. In the CIGS solar cells, theoretical analysis using device simulation was intensively performed to understand device operation mechanism and to design optimum layer configuration to increase efficiency. The decrease in carrier recombination at the buffer/absorber interface is a requirement to obtain high open-circuit voltage (V_{oc}) and thus high efficiency. The interface recombination depends not only on the defect density at the interface, but also more importantly on the conduction band offset (CBO) between the buffer/absorber layers, which is both theoretically supported [16,18,28] and experimentally demonstrated [29–31]. Also, the effect of the CBO is experimentally confirmed in different absorber materials such as $CuInS_2$ [32]

* Corresponding author. Tel./fax: +81 77 561 3065.
E-mail addresses: minemoto@se.ritsumei.ac.jp (T. Minemoto), ro0009he@ed.ritsumei.ac.jp (M. Murata).

http://dx.doi.org/10.1016/j.solmat.2014.10.036
0927-0248/

and SnS [33,34]. In the perovskite solar cells, the absorber is reported to be intrinsic [35] and should be fully depleted. Therefore, not only the CBO of the buffer/absorber layers but also the valence band offset (VBO) of the absorber/HTM layers must be important. Here, we call a blocking layer as buffer from the analogy of the CIGS solar cells. Also, there is an experimental report on the variation of device behaviors with different HTMs [36], which should be partly ascribed to the effect of the band offset. In this study, to understand the operation mechanism and optimum design of the device, we performed theoretical analysis of the effect of the CBO and VBO on the solar cell parameters of the perovskite solar cells with planar junction configuration by SCAPS.

2. Device simulation parameters

We used SCAPS ver. 3.2.01 for simulation platform. The structure of the perovskite solar cell in the simulation is TCO/buffer/interface defect layer 1 (IDL1)/absorber/interface defect layer 2 (IDL2)/HTM. Table 1 summarizes input parameters for each layer. The parameters of TCO, buffer, absorber, and HTM are based on SnO_2:F, TiO_2, $CH_3NH_3PbI_{3-x}Cl_x$, and 2,2',7,7′-tetrakis(N,N-p-dimethoxy-phenylamino)-9,9′- spirobifluorene (Spiro-OMeTAD), respectively. Detailed definition of IDL1 and IDL2 are explained later. Here, N_A and N_D denote acceptor and donor densities, ε_r is relative permittivity, χ is electron affinity, E_g is band gap energy, μ_n and μ_p are mobilities of electron and hole, and N_t is defect density. Exact values of the physics parameters are difficult to obtain, especially for new materials, and we collected and assumed them with our best knowledge in this stage. The thicknesses of TCO, buffer, absorber and HTM were taken from the literature reporting an efficiency of 15.4% [7]. The conduction types of TCO, buffer, absorber and HTM are n^+, n, i (or n^-), p^+, respectively, indicating that the perovskite solar cells is n-i-p junction configuration typically used in amorphous and micro-crystalline silicon solar cells. The perovskite absorber was completely depleted under this parameter set as later shown in the next section, and the absorber depletion was also indicated in the literature [35]. One of the most important parameters to determine the absolute value of the efficiency is the defect density of the absorber. In this study, we assumed $N_t = 2.5 \times 10^{13}$ cm^{-3} to obtain carrier diffusion lengths of electron and hole (L_n and L_p) to be 1 μm, which is a similar value to the experiment [2]. Here, L_n and L_p are identical because all the parameters for the carriers are set to be identical, which is consistent with ambipolar characteristics of the carriers [5]. Other input parameters not included in Table 1 were set to be identical: effective density of states of conduction band and valence band were set to be 2.2×10^{18} and 1.8×10^{19} cm^{-3}, respectively. Thermal velocity of electron and hole was 10^7 cm/s. Defect energy level was the center of band gap and distributed in Gaussian with characteristic energy of 0.1 eV. The defect type was neutral. Capture cross section of electron and hole was 2×10^{-14} cm^2. Pre-factor A_α was 10^5 to obtain absorption coefficient (α) curve calculated by $\alpha = A_\alpha (h\nu - E_g)^{1/2}$. The optical reflectance at the surface and interfaces of each layer is not considered in this simulation.

Fig. 1 shows the current density-voltage (J-V) characteristic of the perovskite solar cell calculated under the parameter set in Table 1. In the figure, quantum efficiency (QE) curve is also shown in inset. The low QE in short wavelength region (< 355 nm) is due to the absorption by SnO_2:F. Here, the CBO of the buffer/absorber and the VBO of the absorber/HTM were set to be zero. The similar ranges of short-circuit current density (J_{sc}) ~22 mA/cm^2 and V_{oc} ~1.0 V with the experimental values [6–9] were successfully obtained, demonstrating that the device simulation can be also used in the perovskite solar cell and the input parameter set was not far from the real device. For further understanding of the device operation mechanism, we examine the effect of the band offsets in the perovskite solar cell.

IDL1 and IDL2 were inserted between the buffer/absorber interface and the absorber/HTM interface, respectively, to take into account interface carrier recombination. Fig. 2 depicts the definition of IDL1 and IDL2 in the case of different band offsets. The band offsets were varied by varying the electron affinity of the buffer and HTM. The signs (positive and negative) of the CBO and VBO were defined from a barrier height for photo-generated carriers. In the case of the CBO of the buffer/absorber interface, electrons generated at the absorber flow to surface side for collection. If the electron affinity of the buffer (χ_{buffer}) is larger than that of the absorber ($\chi_{absorber}$), i.e. the conduction band of the buffer is lower than that of the absorber as shown in Fig. 2(a); energy cliff is formed at the interface and no barrier for the electron is formed. On the other hand, if the conduction band of the buffer is higher than that of the absorber as shown in Fig. 2. (b), energy spike is formed at the interface, which can act as a barrier for electrons. Thus, we defined negative and positive signs of CBO for former and later cases, respectively. In the similar manner, negative and positive signs for VBO were defined as shown in Fig. 2 (c) and (d), respectively. IDL1 was set to consider the carrier recombination between electrons at

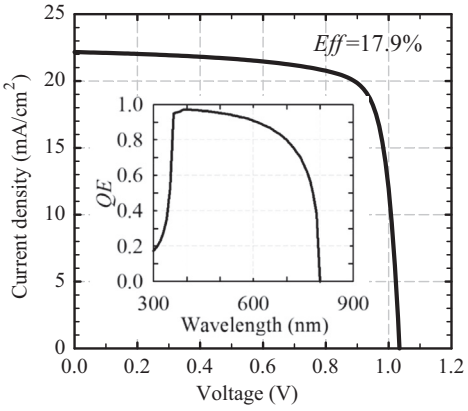

Fig. 1. Simulated J-V characteristic of perovskite solar cell calculated with the parameter set in Table 1. Inset shows the QE curve of the solar cell.

Table 1
Input parameters of device simulation.

Parameter	TCO (SnO_2:F)	Buffer (TiO_2)	Interface defect layer, IDL1	Absorber ($CH_3NH_3PbI_{3-x}Cl_x$)	Interface defect layer, IDL2	HTM (Spiro-OMeTAD)
Thickness (nm)	500	50	10	330	10	350
N_A (cm^{-3})	–	–	–	–	–	2×10^{18} [2]
N_D (cm^{-3})	2×10^{19}	10^{16}	10^{13}	10^{13}	10^{13}	–
ε_r	9.0	9.0	6.5	6.5 [7]	6.5	3.0 [37]
χ (eV)	4.00	3.90 (variable)	3.90 (variable)	3.90 [22]	3.90	2.45 [38] (variable)
E_g (eV)	3.50	3.20	1.55 (variable)	1.55 [3]	1.55 (variable)	3.00 [38]
μ_n / μ_p (cm^2/Vs)	20/10	20/10	2.0/2.0	2.0/2.0 [1]	2.0/2.0	2×10^{-4}/2×10^{-4} [38]
N_t (cm^{-3})	10^{15}	10^{15}	10^{17}	2.5×10^{13}	10^{17}	10^{15}